



Design and synthesis of novel amide AKT1 inhibitors with selectivity over CDK2

Kate S. Ashton^{a,*}, David J. St. Jean Jr.^a, Steve F. Poon^a, Matthew R. Lee^a, John G. Allen^a, Shiwen Zhang^b, Julie A. Lofgren^b, Xiaoling Zhang^b, Christopher Fotsch^a, Randall Hungate^a

^aChemistry Research and Discovery, Amgen Inc., One Amgen Center Drive, Thousand Oaks, CA 91320, USA

^bOncology Research, Amgen Inc., One Amgen Center Drive, Thousand Oaks, CA 91320, USA

ARTICLE INFO

Article history:

Received 4 June 2011

Revised 11 July 2011

Accepted 13 July 2011

Available online 23 July 2011

Keywords:

PKB

AKT

CDK

Cancer

ABSTRACT

Through the analysis of X-ray crystallographic information and previous SAR studies, a novel series of protein kinase B (PKB/AKT) inhibitors was developed. The compounds showed nanomolar inhibition of AKT1 and were selective against cyclin-dependent kinase 2 (CDK2).

© 2011 Elsevier Ltd. All rights reserved.

AKT belongs to the serine/threonine family of kinases and has been the subject of intense anti-cancer research due to its critical role as a regulator of cell growth, differentiation and survival, protein synthesis and metabolism.¹ AKT is part of a metabolic pathway that is frequently dysregulated in a wide variety of cancers through an upstream loss of function mutation in PTEN, or a gain of function mutation in PI3K.² AKT has three major isoforms (AKT1/PKB α , AKT2/PKB β and AKT3/PKB γ) that share >85% homology in the kinase domain. AKT1 is the most widely expressed and activated isoform in tumor cells, and knock-out mice display normal life span phenotype.³ We report herein our efforts thus far to identify kinase-specific modulators of the AKT-pathway.

Initial internal efforts focused on a series of compounds that contained the thiadiazole/thiazole cores shown in Figure 1.^{4–7} These series exhibited excellent potency against AKT1⁸ and PKA enzymes; however had only a 10–17 fold selectivity over CDK2. CDK2 is a serine/threonine kinase that regulates cell cycle transition and cell proliferation,⁹ and as such activity on this kinase was deemed undesirable. In addition PKA is highly homologous to AKT1 in the kinase domain and it was anticipated that selectivity against PKA would translate into a highly selective AKT1 inhibitor. Hence our goal was to improve kinase selectivity while maintaining a favorable off-target profile in a new series of AKT1 inhibitors.

Thus began a search for an analogue that would retain potency and address kinase selectivity. With a plethora of structural information at hand,¹⁰ we decided to move away from the scaffold employed by the previous series and to incorporate rational design

with previous SAR knowledge. The crystal structure of thiadiazole **1** in Figure 2 (residue numbering is based on PKA) is bound to a triple-mutant construct of PKA's kinase domain, that mimics the ATP binding pocket of AKT, and the key interactions are highlighted.¹¹ Analysis of this structure suggested that replacement of the thiadiazole with an amide should conserve the Ala123/Glu121 contact, the amine side chain interactions with Asp184 and Asn171, and the Met173 floor residue contact.

The amide isostere molecule **3** (Fig. 3) retained weak activity for AKT. The drop in potency could be explained by the failure of the amide to fully capitalize on the Lys72 hydrogen bond interaction made by the thiadiazoles/thiazoles. This result however encouraged further paring down of the structure.

It was clear from the crystal structure of **1** that several key residues were being engaged in three distinct areas of the enzyme

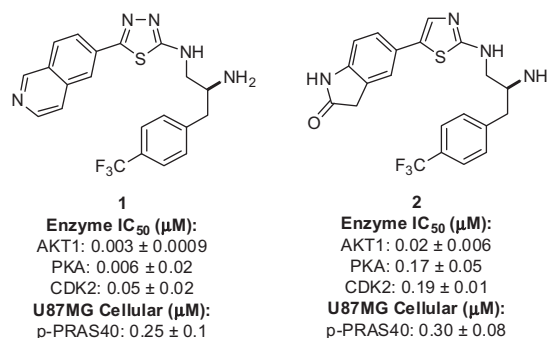


Figure 1. Thiadiazole/thiazole series of AKT1 inhibitors. Data reported as the mean ± SD where $n \geq 3$.

* Corresponding author.

E-mail address: katea@amgen.com (K.S. Ashton).

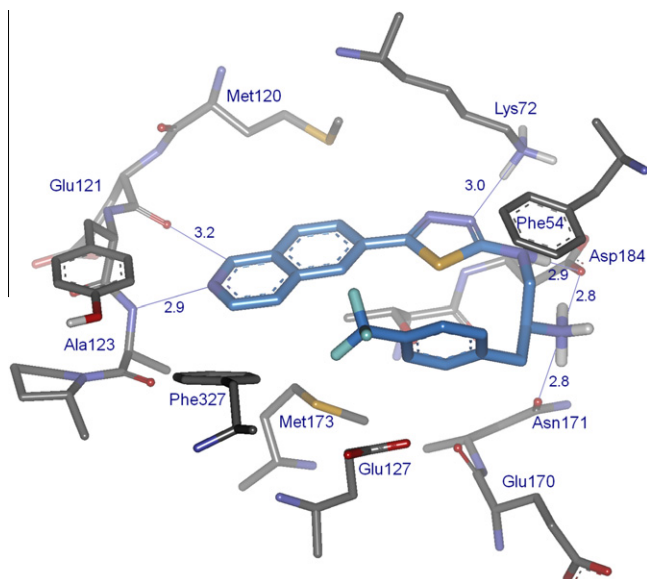


Figure 2. Thiadiazole 1 bound to AKT (PKA triple mutant).

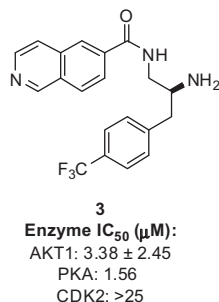


Figure 3. Replacement of heterocyclic core. Data reported as the mean \pm SD where $n \geq 3$.

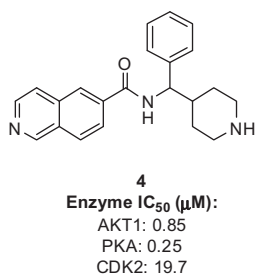


Figure 4. Rationally designed AKT1 inhibitor. Data reported as the mean \pm SD where $n \geq 3$.

pocket and that there was a fourth, as yet unutilized space in the Phe-54 region that could be explored. Therefore it was decided to forego the Met173 floor residue interaction, that in previous series had not imparted significant PKA or CDK2 selectivity, and move away from the 'U-shaped' motif, to incorporate a phenyl ring in the Phe-54 area.

The racemic compound **4** shown (Fig. 4) was initially synthesized based on modeling data that indicated this structure would successfully access the Ala 123/Glu 121 region as well as the Phe-54 region of the protein (see Fig. 5 for a model of a similar structure). The secondary amine was made as literature precedent suggested that this was well tolerated.¹² All of these changes translated into a compound that was surprisingly active on AKT1 and PKA; however, the attractive qualities of this molecule were its structural simplicity and CDK2 selectivity.

With this encouraging result in hand, we investigated the Phe-54 region of the protein to try and improve potency and PKA selectivity with a number of substituted aryl groups (Table 1). Space did not appear to be limited in this region (**5** and **9**), and a range of substitution was well tolerated on the phenyl ring (**10**, **11**, **13**, and **15**). The CDK2 selectivity remained high throughout these changes, however no selectivity over PKA could be achieved through variation in this region of the molecule.

In the next series of molecules we kept the 3,4-dichloro phenyl group constant and turned our attention to modifying the region of the molecule that binds Ala 123/Glu 121. Although this had been previously optimized for the 'U-shaped' thiazoles and thiadiazoles, it was considered that there may have been a slight shift of the molecule in the binding pocket and that this area should be thoroughly re-examined. It had been shown previously that certain groups in this region could impart some PKA selectivity,⁷ and with this in mind a range of heterocyclic bicycles were investigated as shown in Table 2.

It became evident that the 6,6-bicycles imparted the most potency and that of these the isoquinoline was the most active. Selectivity was achieved over PKA with benzoxazolone **19**, however at the expense of AKT1 activity. Further attempts to increase selectivity for AKT1 within the active isoquinoline moiety (**22–25**) were unsuccessful. A strategically placed fluorine (**24**) and methoxy (**22**) were well tolerated but failed to offer any significant selectivity for AKT1 over PKA. All of these compounds retained significant selectivity over CDK2.

Finally, the amine portion of the molecule was examined. Figure 5 shows the binding mode of the amide containing the 3-piperidine ring as predicted by modeling. From this representation it was expected that variation of the amine moiety would be well tolerated due to the many polar residues in this region of the enzyme. The piperidine nitrogen of **27** could engage Glu127/Glu170 as suggested, however the Asp184/Asn171 polar region is also accessible from this scaffold.

Not only did it seem plausible that favorable contacts could arise from various orientations of the amine it also seemed possible to reach the floor of the enzyme. Given that AKT1 contains a methionine (Met173) in this region, whereas PKA contains a leucine in the same position (Leu173), it was thought that by extending a larger group into this region we could exploit this subtle difference. Table 3 summarizes the efforts in this area.

As predicted, variation of the ring size was well tolerated with the 4, 5 and 6-membered rings (**26–29**) being equi-potent. Compound **30** demonstrates that the polar amine group is indeed essential for potent activity and compounds **31** and **32** make the case for retaining the fully saturated ring and basic amine functionality. Substitution of the piperidine nitrogen (**33**, **34**, **35** and **36**) was reasonably well tolerated, indeed the methyl substituted azetidine **36** was equi-potent, but failed to enhance selectivity for AKT1 over PKA. The CDK2 selectivity remained above 50-fold for all of these changes, however there was an increase in CDK2 binding activity moving from the 3- to the 4-piperidine (**26** and **27**), and with the smaller ring size (**R,S-29** and **36**).¹ The synthesis of **R,S-29** is shown in Scheme 1.

The potent affinity for AKT1 and selectivity against CDK2 of these compounds, as well as their ease of synthesis, makes them attractive targets. With regard to the *in vivo* stability of these compounds, the high *in vivo* clearance would require improvement to be of therapeutic use (Table 4).²

¹ The higher CDK2 selectivity achieved with the 3-piperidine ring might be attributed to the amine binding the Glu 127/170 polar region (as is proposed in the model of **27** in Fig. 5) as opposed to the adjacent Asp184 and Asn171 residues.

² The discrepancy between the *in vitro* stability and *in vivo* clearance was not investigated, but the compounds showed high efflux ratios and metabolism by non P450 enzymes was not ruled out by any *in vitro* assays.

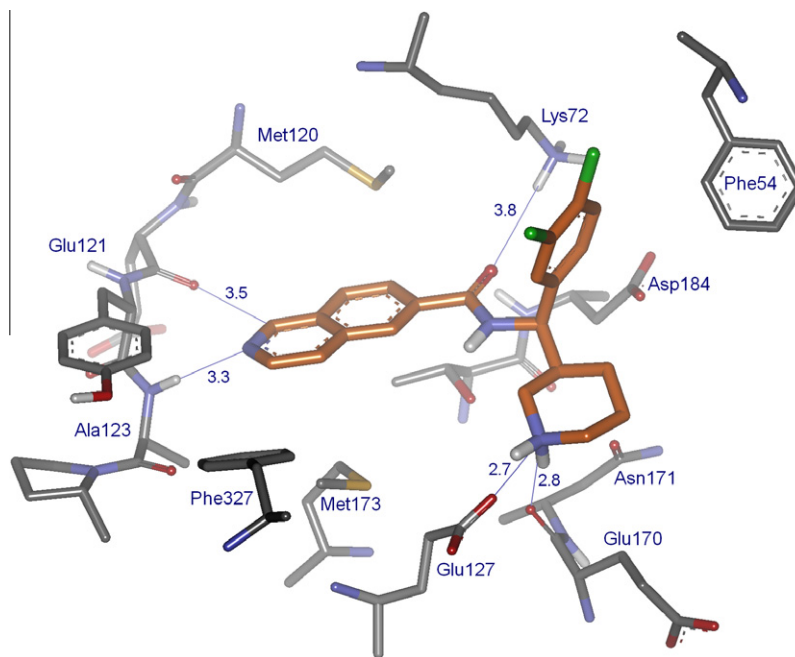
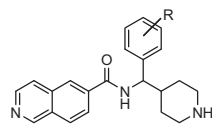


Figure 5. Model of amide 27 in AKT pocket.

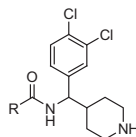
Table 1
Phe-54 region SAR



Cmpd.	Aryl Group	AKT1 IC ₅₀ (μM)	PKA ^a IC ₅₀ (μM)	CDK2 ^a IC ₅₀ (μM)
5		0.40±0.02	0.26	>25
6		1.57 ± 0.06	1.07	>25
7		1.51 ± 0.26	0.13	>25
8		2.68 ± 0.20	0.16	>25
9		0.20 ± 0.01	0.22	>25
10		0.08 ± 0.01	0.16	>25
11		0.07 ± .003	0.03	>25
12		0.19 ± 0.02	0.13	>25
13		0.04 ± 0.004	0.04	>25
14		0.12 ± 0.003	0.10	>25
15		0.04 ± 0.02	0.05	>25
16		0.14 ± 0.01	0.23	>25

Data reported on the racemates as the mean ± SD where $n \geq 3$ except (a) tested once.

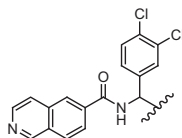
Table 2
Ala 123/Glu 121 Region SAR



Cmpd.	Linker Binder	AKT1 IC ₅₀ (μM)	PKA ^a IC ₅₀ (μM)
17		0.04 ± 0.02	0.05
18		0.35 ± 0.02	1.15
19		0.46 ± 0.04	13.7
20		0.25 ± 0.10	0.29
21 ^b		0.33 ± 0.01	0.85
22		0.039 ± 0.01	0.03
23 ^a		6.85	0.67
24		0.02 ± 0.003	0.09
25		0.14 ± 0.007	0.14

Data reported on the racemates as the mean ± SD where n ≥ 3 except (a) tested once (b) single enantiomer.

Table 3
Amine SAR

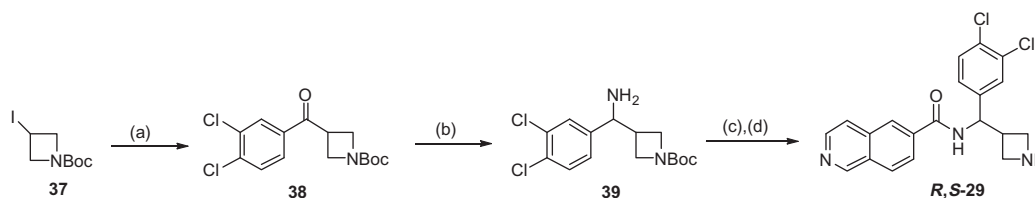


Cmpd.	Amine	AKT1 IC ₅₀ (μM)	PKA ^a IC ₅₀ (μM)	CDK2 ^a IC ₅₀ (μM)
26 ^b		0.04 ± 0.02	0.05	15.6 ± 2.7
27 ^c		0.02 ± 0.0009	0.02	21
28 ^{a,d}		0.03	0.01	>25
(R)-29 ¹³		0.007 ± 0.007	0.01	0.69
(S)-29 ¹³		0.11 ± 0.05	0.03	9.8
30 ^{a,b}		5.80	>25	>25
31 ^b		12.65 ± 1.45	3.41	>25
32 ^b		20.44 ± 1.06	>25	>25

Table 3 (continued)

Cmpd.	Amine	AKT1 IC ₅₀ (μM)	PKAa IC ₅₀ (μM)	CDK2 ^a IC ₅₀ (μM)
33 ^a		2.14	2.01	>25
34 ^a		0.24	0.39	>25
35		2.30 ± 0.23	0.98	>25
36		0.007 ± 0.003	0.01	0.36

Data reported on the single enantiomer as the mean ± SD where $n \geq 3$ except (a) tested once (b) racemic (c) cis diastereomers only (d) mixture of four diastereomers.



Scheme 1. Synthesis of **29**. Reagents and conditions: (a) activated Zn, 1,2-dibromoethane, THF, 65 °C; CuCN, LiCl, 3,4-dichlorobenzoyl chloride, -10 °C to rt, quant,¹⁴; (b) NH₄OAc, NaCNBH₄, MeOH, 75 °C, 70%, (c) HATU, Hung's base, isoquiniline-6-carboxylic acid, DMF, rt, (d) HCl, MeOH, rt, 20% over 2 steps.

Table 4
Selected in vivo and in vitro data

Cmpd.	Structure	AKT1 (IC ₅₀ μM)	PKA ^a (IC ₅₀ μM)	CDK2 ^a (IC ₅₀ μM)	p-Pras40 ^a (IC ₅₀ μM)	RLM ^a (% turnover)	HLM ^a (% turnover)	In Vivo Rat CL ^a (L/h/kg)
(R)-29		0.007 ± 0.007	0.01	0.68	0.24	33.4	10.9	10.4
24		0.02 ± 0.003	0.03	>25	0.39	15.9	10	3.5

Data reported as the mean ± SD where $n \geq 3$ except (a) tested once.

In conclusion a novel series of structurally simple amides has been developed through consideration of previously learned SAR and structure based design. The compounds display excellent potency on AKT1 and PKA and selectivity against CDK2.

Acknowledgments

The authors are indebted to the PKDM team for in vivo work, and to Tisha San Miguel and John McCarter for additional in vitro screening.

A. Supplementary data

Supplementary data associated with this article can be found, in the online version, at [doi:10.1016/j.bmcl.2011.07.056](https://doi.org/10.1016/j.bmcl.2011.07.056).

References and notes

- (a) Lindsley, C. W.; Barnett, S. F.; Layton, M. E.; Bilodeau, M. T. *Curr. Cancer Drug Target* **2008**, *8*, 7; (b) Li, Q. *Expert Opin. Ther. Pat.* **2007**, *17*, 1077; (c) Heerding, D. A.; Safonov, I. G.; Verma, S. K. *Annu. Rep. Med. Chem.* **2007**, *42*, 365.
- (a) Hennessy, B. T.; Smith, D. L.; Ram, P. T.; Lu, Y.; Mills, G. B. *Nat. Rev. Drug Discovery* **2005**, *4*, 988; (b) Bader, A. G.; Khang, S.; Zhao, L.; Vogt, P. K. *Nat. Rev. Cancer* **2005**, *5*, 921; (c) Testa, J. R.; Bellacosa, A. *Proc. Natl. Acad. Sci. U.S.A.* **2001**, *98*, 10983; (d) Cully, M.; You, H.; Levine, A. J.; Mak, T. W. *Nat. Rev. Cancer* **2006**, *6*, 184.
- Dummler, B.; Hemmings, B. A. *Biochem. Soc. Trans.* **2007**, *35*, 231.
- AKT1, PKA, and CDK2 enzymatic activity was measured using a previously described method. Zhang, X. L.; Zhang, S. W.; Yamane, H.; Wahl, R.; Ali, A.; Lofgren, J. A.; Kendall, R. L. *J. Biol. Chem.* **2006**, *281*, 13949.
- U87MG cells in 5% FBS media were incubated with inhibitors in threefold serial dilutions for 1h at 37 °C. The cells were lysed and PRAS40 phosphorylation was quantified by ELISA assay. Phospho-PRAS40 was normalized to total PRAS40. Kovacina, K. S.; Park, G. Y.; Bae, S. S.; Guzzetta, A. W.; Schaefer, E.; Birnbaum, M. J.; Roth, R. A. *J. Biol. Chem.* **2003**, *278*, 10189.
- Zeng, Q.; Bourbeau, M. P.; Wohlhieter, G. E.; Yao, G.; Monenschein, H.; Rider, J. T.; Lee, M. R.; Zhang, S.; Lofgren, J. A.; Freeman, D. J.; Li, C.; Tominey, E.; Huang, X.; Hoffman, D.; Yamane, H. K.; Tasker, A. S.; Dominguez, C.; Viswanadha, V. N.; Hungate, R.; Zhang, X. *Bioorg. Med. Chem. Lett.* **2010**, *20*, 1652–1656.
- Zeng, Q.; Allen, J. G.; Bourbeau, M. P.; Wang, X.; Yao, G.; Tadesse, S.; Rider, J. T.; Yuan, C. C.; Hong, F.-T.; Lee, M. R.; Zhang, S.; Lofgren, J. A.; Freeman, D. J.; Yang, S.; Li, C.; Tominey, E.; Huang, X.; Hoffman, D.; Yamane, H. K.; Fotsch, C.; Dominguez, C.; Hungate, R.; Zhang, X. *Bioorg. Med. Chem. Lett.* **2010**, *20*, 1559–1564.
- AKT1 was the only AKT isoform routinely tested against as it is thought to be the major isoform contributing to oncogenic activity. Dummler, B.; Hemmings, B. A. *Biochem. Soc. Trans.* **2007**, *35*, 231. In addition all other isoforms of AKT potency tracked well with AKT1 upon testing.

9. Besson, A.; Dowdy, S. F.; Roberts, J. M. *Dev. Cell* **2008**, *14*, 159.
10. Davies, T. D.; Verdonk, M. L.; Graham, B.; Saalau-Bethell, S.; Hamlett, C. C. F.; McHardy, T.; Collins, I.; Garrett, M. D.; Workman, P.; Woodhead, S. J.; Jhoti, H.; Barford, D. *J. Mol. Biol.* **2007**, *367*, 882; For a description of a similar crystallography strategy see: Caldwell, J. J.; Davies, T. G.; Donald, A.; McHardy, T.; Rowlands, M. G.; Aherne, G. W.; Hunter, L. K.; Taylor, K.; Ruddle, R.; Raynaud, F. I.; Verdonk, M.; Workman, P.; Garrett, M. D.; Collins, I. *J. Med. Chem.* **2008**, *51*, 2147.
11. Mutations: PKA Val123 was mutated to AKT Ala, and PKA Leu173 was mutated to AKT Met. Additionally, PKA Lys181 was mutated to AKT Gln, but this residue faces away from the ATP binding pocket. Gassell, M.; Breitenlechner, C. B.; Ruger, P.; Jucknischke, U.; Schnieder, T.; Huber, R.; Bossemeyer, D.; Engh, R. A. *J. Mol. Biol.* **2003**, *329*, 1021.
12. (a) Saxty, G.; Woodhead, S. J.; Berdini, V.; Davies, T. G.; Verdonk, M. L.; Wyatt, P. G.; Boyle, R. G.; Barford, D.; Downham, R.; Garrett, M. D.; Carr, R. A. *J. Med. Chem.* **2007**, *50*, 2293–2296; (b) Lipka, B.; Pan, G.; Corbett, M.; Li, C.; Kauffman, G. S.; Pandit, J.; Robinson, S.; Wei, L.; Kozina, E.; Marr, E. S.; Borzillo, G.; Knauth, E.; Barbacci-Tobin, E. G.; Vincent, P.; Troutman, M.; Baker, D.; Rajamohan, F.; Kakar, S.; Clark, T.; Morris, J. *Bioorg. Med. Chem. Lett.* **2008**, *18*, 3359–3363.
13. The absolute configuration of the azetidines was determined by Mosher ester analysis – see [Supplementary data](#).
14. Billotte, S. *Synlett* **1998**, *4*, 379–380.